Numerical Study on the Effect of Buoyancy Force on Single Phase Thermal Stratification in both Cold Legs and Downcomer by Emergency Core Cooling System Injection

Gong Hee Lee [a,b*], Ae Ju Cheong [a]
[a]*Nuclear Safety Research Department, Korea Institute of Nuclear Safety, Daejeon, 34142, Korea*
[b]*Nuclear and Radiation Safety Department, University of Science and Technology, Daejeon 34133, Korea*
[*]*Corresponding author: ghlee@kins.re.kr*

1. Introduction

PTS (pressurized thermal shock) phenomenon is characterized by multi-dimensional and non-equilibrium flow conditions. For example, in case ECCS (emergency core cooling system) is operated during LOCA (loss of coolant accident) in a PWR (pressurized water reactor), PTS phenomenon occurs as cooling water is injected into a cold leg, mixed with the hot primary coolant, and then entrained into a reactor vessel. Insufficient flow mixing may cause temperature stratification and steam condensation. In addition, flow vibration may cause thermal stresses in the surrounding structures, which reduce the life of the reactor vessel. Because of this importance, the effect of PTS has been actively studied either experimentally or numerically [1]. Among these, the ROSA project [2,3] undertaken by the OECD/NEA includes six types of the separate or the integral effect tests. In this study, the calculation with ANSYS CFX R.17 [4] was performed for the Test 1 『Temperature stratification and coolant mixing in unsteady state during emergency core cooling system injection』 and then the predicted results were compared with the measured data.

Additionally, because temperature difference between the hot coolant at the inlet of the cold leg and the cold cooling water at the inlet of the ECCS injection line is 200 K or more, buoyancy force due to the density difference may have the significant effect on the thermal-hydraulic characteristics of flow. Therefore, in this study, effect of buoyancy force on single phase thermal stratification in both cold legs and downcomer by the ECCS injection was numerically studied.

2. Analysis model

The objective of Test 1 is to clarify the phenomenon of temperature stratification on the cold legs and the upper region of downcomer of the reactor vessel, which are important for the evaluation of PTS during the coolant injection by the ECCS, and to obtain the measured data for the main parameters with the aim of validating the simulation code and the numerical modeling. Fig. 1 shows the schematic diagram of the analysis model.

Test 1-1 (ST-NC-34 in JAEA) was performed as a separate effect test. The primary and secondary pressures under the single-phase natural circulation operating conditions were 15.5 MPa and 6.7 MPa, respectively, and the water level in the primary loop was maintained at 100% level. An inner diameter of a cold leg was 207 mm. The ECCS lines attached to the cold legs have different installation types and locations. While the ECCS line A was installed perpendicularly to the cold leg A, the ECCS line B formed a 45° angle with the cold leg B.

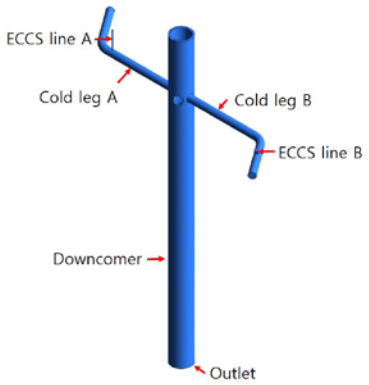

Fig. 1. Computational domain.

As shown in Fig. 3, Fig. 4 and Fig. 5 (a), to investigate the thermal stratification phenomenon in the cold leg, 21 thermocouples were installed in 3 columns and 7 rows at two cross sections (TE2, TE3) in the cold leg between the ECCS line A and the downcomer. Meanwhile, as shown in Fig. 6 (a), to examine the thermal stratification phenomenon in the downcomer, 18 thermocouples were installed. The nominal accuracy of the thermocouple measurements is ± 2.75 K.

In this study, the measured and the calculated results were compared for the cases where the cold coolant was injected through the ECCS line A during time intervals of 18 s ~ 100 s under the natural circulation condition after the main coolant pump stopped.

3. Numerical modeling

3.1 Consideration of Buoyancy Force in the Governing Equations

According to the ANSYS CFX-Solver theory guide [5], the Reynolds averaged momentum equation is

$$\frac{\partial \rho U_i}{\partial t}+\frac{\partial}{\partial x_j}\left(\rho U_i U_j\right)=-\frac{\partial p'}{\partial x_i}+\frac{\partial}{\partial x_j}\left[\mu_{eff}\left(\frac{\partial U_i}{\partial x_j}+\frac{\partial U_j}{\partial x_i}\right)\right]+S_M \quad (1)$$

where S_M is the sum of body forces (including buoyancy force), μ_{eff} is the effective viscosity accounting for turbulence, and p' is the modified pressure. The $k-\varepsilon$ model is based on the eddy viscosity concept and thus

$$\mu_{eff} = \mu + \mu_t \tag{2}$$

where μ_t is the turbulence viscosity. The $k-\varepsilon$ model assumes that μ_t is coupled to the turbulence kinetic energy (k) and turbulence eddy dissipation (ε) via the following relation:

$$\mu_t = \rho C_\mu \frac{k^2}{\varepsilon} \tag{3}$$

where C_μ is a constant.

The values of k and ε come directly from the following differential transport equations for k and ε.

$$\frac{\partial(\rho k)}{\partial t} + \frac{\partial}{\partial x_j}\left(\rho U_j k\right) = \frac{\partial}{\partial x_j}\left[\left(\mu + \frac{\mu_t}{\sigma_k}\right)\frac{\partial k}{\partial x_j}\right] + P_k - \rho\varepsilon + P_{kb} \tag{4}$$

$$\frac{\partial(\rho\varepsilon)}{\partial t} + \frac{\partial}{\partial x_j}\left(\rho U_j \varepsilon\right) = \frac{\partial}{\partial x_j}\left[\left(\mu + \frac{\mu_t}{\sigma_\varepsilon}\right)\frac{\partial \varepsilon}{\partial x_j}\right] + \frac{\varepsilon}{k}\left(C_{\varepsilon 1}P_k - C_{\varepsilon 2}\rho\varepsilon + C_{\varepsilon 1}P_{\varepsilon b}\right) \tag{5}$$

In Equation (4), P_k is the turbulence production due to the viscous forces. P_{kb} and $P_{\varepsilon b}$ represent the influence of the buoyancy forces, and if the full buoyancy model is used, these terms are modeled as follows.

$$P_{kb} = -\frac{\mu_t}{\rho\sigma_\rho}\frac{\partial \rho}{\partial x_i} g_i \tag{6}$$

$$P_{\varepsilon b} = C_3 \cdot \max\left(0, P_{kb}\right) \tag{7}$$

where turbulence Schmidt number, $\sigma_\rho = 1.0$, and dissipation coefficient, $C_3 = 1.0$. Here $P_{\varepsilon b}$ is assumed to be proportional to P_{kb} and must be positive.

Table I: Test cases classified by either including or excluding buoyancy force terms in the momentum and turbulence transport equations.

	Case1	Case2	Case3
Momentum eq.	×	●	●
Turbulence Transport eq.	×	×	●

In this study, to investigate the effect of buoyancy force on single phase thermal stratification in both cold legs and downcomer by the ECCS injection, three test cases were considered, as shown in Table I. For case1, the effect of buoyancy force was not considered. For case2, the effect of buoyancy force was only considered in the momentum equation. For case3, the effect of buoyancy force was considered in both the momentum equation and turbulence transport equations.

3.2 Grid System and Boundary Conditions

Fig. 2 shows the grid system, generated by using ICEM-CFD software, for the computational domain that had the same size as the test facility.

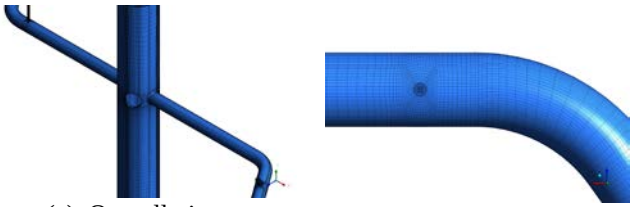

(a) Overall view (b) ECCS A

Fig. 2. Grid system.

The grid shape was hexahedral, and the total number of grid points used in the calculation was 9.44×10^5. In the computational domain, the maximum y^+ was about 458, and its location was near the region where the inner wall of the pressure vessel and the hot leg were bordered.

The measured unsteady flow rate and temperature were applied at inlet of the cold leg A/B and the ECCS injection line A. For reference, the temperature difference between the hot coolant at the inlet of the cold leg A/B and the cold cooling water at the inlet of the ECCS injection line A was 200 K or more. On the other hand, the turbulence intensity at each inlet was assumed to be 5.0%. The average static pressure condition was applied at the outlet. No-slip and adiabatic conditions were applied at all wall interfaces including the reactor vessel.

3.3 Numerical Model

In this study, the turbulent flow field inside the ROSA/LSTF (Large Scale Test Facility) was calculated under unsteady, single-phase, incompressible and non-isothermal conditions by using the commercial computational fluid dynamics software ANSYS CFX R.17. High resolution scheme with quasi-second-order accuracy was used for the convection-terms-of-momentum and -turbulence equations. The second order backward Euler option, the default implicit time step method with the second order accuracy in ANSYS CFX R.17, was used as the time discretization scheme. For the calculation of the unsteady flow, the calculation was performed up to the flow development time of 200 s with a time step of 0.1 s. It was determined that the solution was converged when the root mean square residuals of the individual equations were 10^{-5} or less at each time step.

As explained in the section 3.1, standard $k-\varepsilon$ model was used to simulate the turbulent flow inside the ROSA/LSTF. To model the flow in the near-wall region, the scalable wall function method was applied.

4. Results and Discussion

4.1 General thermal flow characteristics

Fig. 3 shows the streamline of the cold cooling water injected at inlet of the ECCS injection line A and the distribution of fluid temperature at the measurement sections (TE2, TE3) of the cold leg A.

When considering the effect of buoyancy force (case2 & case3), cold cooling water injected at the inlet of the ECCS injection line A moved toward the lower part of the cold leg A and then flow mixing with the hot coolant occurred. The mixed flows proceeded along the cold leg A and then entered into the downcomer along the outer wall of the pressure vessel. On the other hand, when not considering the effect of buoyancy force (case1), cold cooling water injected at the inlet of the ECCS injection line A could not move toward the lower part of the cold leg A and still maintained its position at the upper part of the cold leg A. In addition, the flow mixing between the hot coolant and cold cooling water was not active in comparison with the cases considering the effect of buoyancy force (case2 & case3).

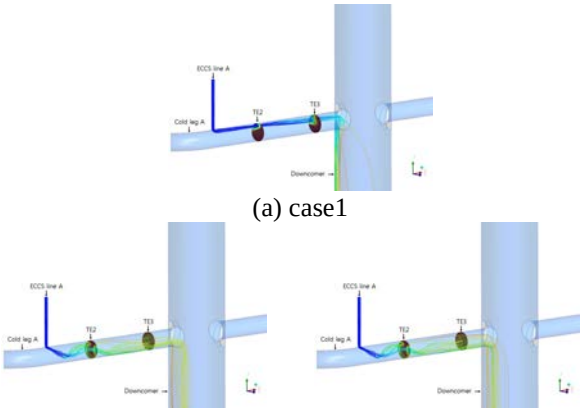

(a) case1

(b) case2 (c) case3

Fig. 3 Streamlines and contours of fluid temperature at cross-sectional plane TE2 and TE3 of the cold leg A (at t=60s)

To identify the thermal stratification region, wall surface temperature distribution was shown in Fig. 4. When considering the effect of buoyancy force (case2 & case3), the strongest thermal stratification was found at the location where the cold cooling water injected at the inlet of the ECCS injection line A contacted with the lower part of the cold leg A. In addition, as previously explained in Fig. 3, because the mixed flow moved along the lower part of the cold leg A and then entered into the downcomer along the outer wall of the pressure vessel, the thermal stratification phenomena occurred in these regions. On the other hand, when not considering the effect of buoyancy force (case1), the significant thermal stratification was not found at the lower part of the cold leg A.

4.2 Comparison of fluid temperature distribution in the cold leg A

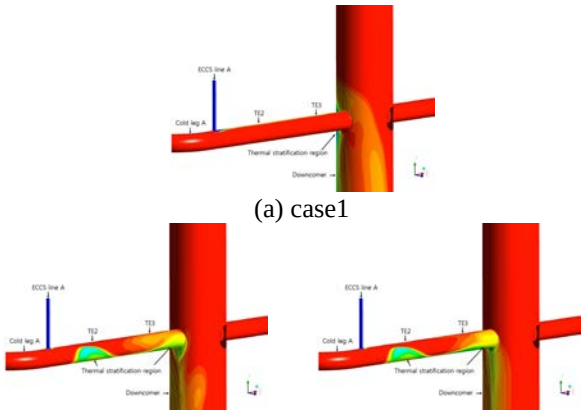

(a) case1

(b) case2 (c) case3

Fig. 4 Contour of wall surface temperature to demonstrate the thermal stratification region at t=60 s

Fig. 5 shows a comparison of the calculated and the measured temperature at three locations (TE3A4, TE3B4, TE3C4) in the cold leg A section (TE3) where are 0.7465 m from the pressure vessel center. The section (TE3) is located further away from the ECCS injection line A in the downstream direction (closer to the pressure vessel) in comparison with the section (TE2) shown in Fig. 3 and Fig. 4. Therefore, it is expected that more flow mixing between the cold cooling water injected at the inlet of the ECCS injection line A and the hot coolant occurs in comparison with the section (TE2), and, as a result, the measured temperature at three positions of the section (TE3) showed similar unsteady behaviors during the ECC water injection period.

For case2 where the effect of buoyancy force was only considered in the momentum equation, the predicted fluid temperature was relatively in good agreement with the measured data during the ECC water injection period. For case3 where the effect of buoyancy force was considered in both the momentum equation and turbulence transport equations, ANSYS CFX over-predicted fluid temperature at TE3C4 compared to the measured data during the ECC water injection period. For case1 where the effect of buoyancy force was not considered, ANSYS CFX could not consider the unsteady temperature behaviors at TE3A4 and under-predicted fluid temperature at TE3C4 compared to the measured data during the ECC water injection period.

Due to the non-disclosure limitations of measurement data, quantitative values of the fluid temperature corresponding to the vertical axis of the graph were not specified.

4.3 Comparison of fluid temperature distribution in the downcomer

Fig. 6 shows a comparison of the calculated and measured temperature measurements for six locations (TE4A12/22, TE4B12/22, TE4C12/22) in the mid-plane of the downcomer where are 0.277 m from the center of the pressure vessel.

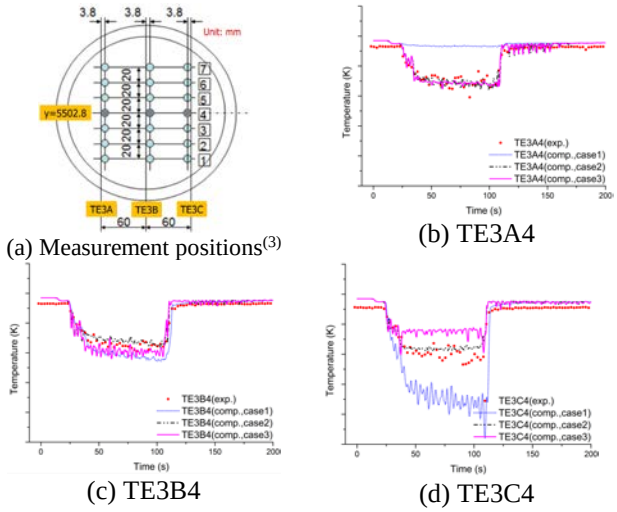

(a) Measurement positions[3] (b) TE3A4

(c) TE3B4 (d) TE3C4

Fig. 5 Time-dependent variation of fluid temperature at cross-sectional plane TE3 in the cold leg A

For case1 where the effect of buoyancy force was not considered, ANSYS CFX could not consider the unsteady temperature behaviors at six locations during the ECC water injection period. Although case 3 improved the prediction accuracy for the fluid temperature distribution in the downcomer by considering the effect of buoyancy force in turbulence transport equations, it could not guarantee the superiority over case 2 at all measured locations, as shown in Fig. 6(c).

5. Conclusions

In this study, the calculation with ANSYS CFX R.17 was performed for the ROSA/LSTF Test 1 and then the predicted results were compared with the measured data. Additionally, effect of buoyancy force on single phase thermal stratification in both cold legs and downcomer by the ECCS injection was numerically studied. The main conclusions are as follows: (1) ANSYS CFX could reasonably predict flow mixing and thermal layer phenomena between cold cooling water injected from the ECCS injection pipe and hot coolant in the cold leg by at least inclusion of the buoyancy force term in the momentum equation. (2) Because considering the effect of buoyancy force in turbulence transport equations could not always improve the prediction accuracy for the fluid temperature distribution in the full computational domain, licensing applicant using ANSYS CFX should conduct the sensitivity study to evaluate whether the consideration of the buoyancy force effect in turbulence transport equations can give the physically reasonable result.

ACKNOWLEDGEMENT

This work was supported by the Nuclear Safety Research Program through the Korea Foundation Of Nuclear Safety (KOFONS), granted financial resource from the Nuclear Safety and Security Commission (NSSC), Republic of Korea (No. 1305002). This paper was also written by using the experimental data from OECD/NEA ROSA Project (CSNI2009/01).

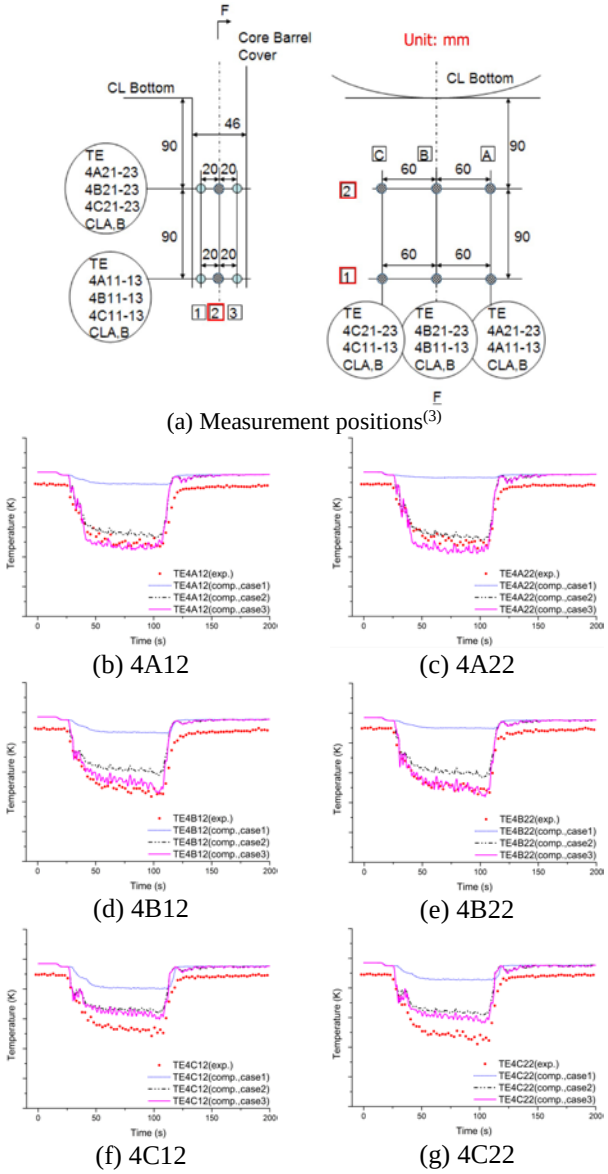

(a) Measurement positions[3]

(b) 4A12 (c) 4A22

(d) 4B12 (e) 4B22

(f) 4C12 (g) 4C22

Fig. 6 Time-dependent variation of fluid temperature at several measurement points in the downcomer

REFERENCES

[1] T. Farkas, and I. Toth, Fluent Analysis of a ROSA Cold Leg Stratification Test, Nuclear Engineering and Design, Vol.240, p. 2169, 2010.
[2] H. Nakamura, T. Watanabe, T. Takeda, Y. Maruyama, and M. Suzuki, Overview of Recent Efforts through ROSA/LSTF Experiments, Nuclear Engineering and Technology, Vol.41, p. 753, 2009.
[3] Final Data Report of OECD/NEA ROSA Project Test 1-1, Japan Atomic Energy Agency, 2008.
[4] ANSYS CFX, Release 17, ANSYS Inc.
[5] ANSYS CFX-Solver theory guide, ANSYS Inc.